









Bicortical screw placement and microdamage in medial buttress plates in the management of Pauwels type III femoral neck fractures: A scanning electron microscopy-based analysis

Osman Gorkem Muratoglu, MD¹ , Cem Yildirim, MD¹ , Hasan Ceylan, MD¹ , Yinal Neşes Huvaj, MSc² , Mehmet Demirel, MD³ , Süreyya Ergün Bozdağ, PhD⁴ 

¹Department of Orthopedics and Traumatology, Cam and Sakura City Hospital, İstanbul, Türkiye

²Department of Geological Engineer, Turkish Petroleum Corporation, Ankara, Türkiye

³Department of Orthopedics and Traumatology, İstanbul University Faculty of Medicine, İstanbul, Türkiye

⁴Department of Mechanical Engineer, İstanbul Technical University, Mechanical Engineering Faculty, İstanbul, Türkiye

Displaced femoral neck fractures (FNFs) in young adults are most likely to result from high-energy trauma. According to the Pauwels classification, these fractures in younger patients commonly occur as vertically oriented, biomechanically unstable type III FNFs, require precise anatomical reduction and rigid internal fixation.^[1] The predominant vertical shear forces in type III FNFs make stable fixation technically demanding and prone to complications such as fixation failure, nonunion, and avascular necrosis. Due to these biomechanical

ABSTRACT

Objectives: This study aims to investigate the microstructural effects of distal bicortical screw placement in medial buttress plate (MBP) constructs using scanning electron microscopy (SEM).

Materials and methods: Ten synthetic femur models with standardized Pauwels type III fractures were divided into two groups. All specimens received fixation with three cannulated screws in an inverted triangle configuration. Group A received a MBP fixed with four unicortical screws. Group B received the same construct, except for the most distal screw was inserted bicortically. All specimens underwent combined axial and torsional cyclic loading, followed by load-to-failure testing. Plates were, then, analyzed under SEM to assess deformation and microdamage. A semi-quantitative scoring system was used to compare the severity of microstructural changes between groups.

Results: The SEM analysis revealed significantly more microdamage in Group B compared to Group A (median deformation scores: 4 vs. 2; $p=0.0181$). Plates with bicortical screw placement showed localized plastic deformation, microcracks, and in some cases, complete fractures, particularly at the bent midsection of the plate. In contrast, unicortical plates showed only mild surface irregularities without structural failure.

Conclusion: Although distal bicortical screw placement may enhance initial mechanical stability, it also increases the risk of microstructural damage in MBPs, potentially compromising long-term durability. These findings underscore the importance of optimizing screw configuration to balance stability with implant longevity in the treatment of vertically unstable femoral neck fractures.

Keywords: Femoral neck fracture, medial buttress plate, microstructural damage, scanning electron microscopy, vertically unstable.

Received: June 26, 2025

Accepted: August 19, 2025

Published online: September 12, 2025

Correspondence: Cem Yildirim, MD, Cam ve Sakura Şehir Hastanesi, Ortopedi ve Travmatoloji Kliniği, 34480 Başakşehir, İstanbul, Türkiye.

E-mail: cemyildirim701@hotmail.com

Doi: 10.52312/jdrs.2026.2457

Citation: Muratoglu OG, Yildirim C, Ceylan H, Huvaj YN, Demirel M, Ergün Bozdağ S. Bicortical screw placement and microdamage in medial buttress plates in the management of Pauwels type III femoral neck fractures: A scanning electron microscopy-based analysis Jt Dis Relat Surg 2026;37(1):209-217. doi: 10.52312/jdrs.2026.2457.

©2026 All right reserved by the Turkish Joint Diseases Foundation

This is an open access article under the terms of the Creative Commons Attribution-NonCommercial License, which permits use, distribution and reproduction in any medium, provided the original work is properly cited and is not used for commercial purposes (<http://creativecommons.org/licenses/by-nc/4.0/>).

challenges and the high risk of adverse outcomes, the surgical management of type III FNFs remains particularly difficult.^[2] The optimal fixation strategy for FNFs remains a matter of ongoing debate in orthopedic surgery. Over the years, various methods have been utilized, including multiple cannulated screws, sliding hip screw, and newer constructs such as fixed-angle locking plates.^[3-5]

Currently, the configuration of three cannulated screws placed parallel to the longitudinal axis of the femoral neck are the most widely applied method in clinical practice, owing to its minimally invasive nature, technical simplicity, and capacity to deliver dynamic interfragmentary compression.^[1,2,6] However, a major drawback of this technique is its susceptibility to failure in vertically oriented fractures, where shear forces dominate. Reported failure rates with parallel screw fixation range from 10 to 30%, with complications such as screw back-out, nonunion, and osteonecrosis of the femoral head.^[7,8] To address this drawback, Mir and Collinge^[9] proposed augmenting internal fixation with a medial buttress plate (MBP, typically a one-third semi-tubular plate) for vertically oriented FNFs. This concept draws on the use of buttress (or “anti-glide”) plating to stabilize fractures, such as those of the proximal tibia or distal radius, that are similarly challenged by shear forces and require resistance to axial loading to maintain stability.^[10,11] Recent biomechanical^[12,13] and clinical^[14,15] studies have demonstrated that augmenting cannulated screws with a MBP provides superior stability and higher union rates compared to screw fixation alone. As a result, this combination has gained increasing attention in the treatment of type III FNFs in young patients.

The analysis of crack growth has been studied from many scientific perspectives, including biomechanical effects, fracture mechanics, image analysis, and materials engineering.^[16] However, there is no other study in the literature examining whether the screws (single cortical or double cortical) used in the application of the MBP against axial resistance in Pauwels type III FNFs cause deformation on the plate.

Previous biomechanical studies have primarily demonstrated that MBP augmentation increases construct stiffness and improves resistance to vertical loading in Pauwels type III FNFs.^[9,12,14] However, in our prior experimental study,^[2] we observed that multiple cannulated screw configurations, particularly the inverted triangle setup, could offer sufficient torsional stability

even in the absence of MBP augmentation. More interestingly, although distal bicortical screw placement within the MBP appeared to enhance axial stability, it did not significantly improve rotational resistance. These findings suggest that the role of MBP in overall construct performance may be more nuanced than previously thought. The analysis of crack growth has been investigated from various scientific perspectives, including biomechanics, fracture mechanics, image analysis, and materials engineering.^[16] However, no study has specifically evaluated whether the screws (single or double cortical) used in MBP application against axial resistance in Pauwels type III FNFs cause deformation of the plate. Despite growing interest in this technique, there remains a lack of microstructural data examining how these plates deform or fail under physiological loading conditions. In particular, the local biomechanical consequences of distal bicortical screw placement at the plate-bone interface have not been systematically investigated. Bridging these gaps may lead to more effective implant designs and improved fixation strategies for managing vertically unstable FNFs.

In the present study, we aimed to evaluate the deformation patterns of MBPs under both axial and torsional loads, using scanning electron microscopy (SEM). These plates were previously utilized in a biomechanical investigation of fixation strategies for displaced FNFs.^[2] Our first hypothesis was that MBP would maintain structural integrity and provide mechanical support under combined axial and torsional stress conditions. The second hypothesis was that these plates would exhibit localized deformation, particularly at the bent region, as a result of shear forces being redirected into compressive loads at the point of bending.

MATERIALS AND METHODS

Sample preparation and test setup

The biomechanical part of this study was conducted at the İstanbul Technical University Biomechanics Laboratory, and the SEM analysis was performed at the Turkish Petroleum Company between September 2021 and October 2021. This study was designed as an experimental investigation involving only biomechanical testing and scanning electron microscopy (SEM) analysis. As it did not involve human or animal subjects, ethical committee approval was not required.

Two experimental groups were defined to evaluate the structural behavior of MBPs

following biomechanical loading. A total of 10 third-generation composite femora (FMR-01 New Third Generation Composite Left Femur, Selbones Research Lab., Kayseri, Türkiye) were used, with five specimens assigned to each group. A Pauwels type III fracture pattern was created in each sample by a standardized osteotomy at a 70° angle to the horizontal plane in the middle third of the femoral neck based on the method of Giordano et al.^[17] The composite femur models used in that study and the present analysis have been validated, with trabecular hardness values estimated at 69.1% of human cortical bone, supporting their suitability for biomechanical evaluation.^[18,19]

Fixation was performed using three partially threaded 6.5-mm cannulated screws with 32 mm distal threads (TST™ Medical Devices, Istanbul, Türkiye), inserted over pre-positioned 2.5-mm guide pins using a 4.5-mm cannulated drill bit. The screws were arranged in an inverted triangle configuration, with two screws placed inferiorly and one superiorly in the femoral neck and advanced up to 5 mm from the subchondral surface of the femoral head. Washers were not used in any specimen.

In Group A (n=5), a four-hole MBP (Response Ortho, Istanbul, Türkiye) was applied to the medial aspect of the femoral neck and fixed with four 3.5-mm non-locking cortical screws, all of which, including the most distal screw, were inserted unicortically. In Group B (n=5), the same fixation construct was used, except that the most distal

screw was inserted bicortically, while the remaining three were unicortical (Figure 1). All materials utilized in the experiment consisted of single-use implant sets approved (EU approved) for surgical application.

Following anatomic reduction and fixation, each femur was sectioned at the mid-diaphysis to minimize tensile bending forces during mechanical testing. The specimens were then embedded in cylindrical molds (50 mm in diameter, 50 mm in depth) using polyester paste (Politek®, Istanbul, Türkiye). To assess the mechanical integrity of each construct, all specimens were subjected to combined axial and torsional cyclic loading, followed by static load-to-failure testing. Cyclic loading was applied using a servohydraulic materials testing machine (MTS 858 Mini Bionix II, Eden Prairie, MN, USA) to simulate physiological loading conditions of the hip joint during gait. Each specimen was loaded with an axial compression force ranging from 60 N to 600 N at a frequency of 2.5 Hz, while simultaneously applying a torsional load ranging from 0.7 Nm to 7 Nm, for a total of 500 cycles. The 600 N axial load and 7 Nm (500 cycles) torsional moment did not approach the structural failure thresholds of the structures. These loading parameters were derived from preliminary testing and were carefully maintained within the elastic range of the materials. These values were obtained by applying pre-tests according to the constructs we used in this study.

Following dynamic loading, static load-to-failure testing was conducted by resetting all loads and applying displacement-controlled loading at a constant rate of 1.8 mm/min in the axial direction and 4.5°/min in rotation. Load-to-failure was defined by the occurrence of at least one of the following failure criteria:

- A sudden decrease in the load as observed on the force-displacement curve
- Fracture at any site of the specimen
- Displacement exceeding 10 mm at the fracture site
- Visible plastic deformation of the MBP
- Screw loosening or displacement

Scanning electron microscopy procedure

The MBPs examined in the current study were retrieved from specimens which previously underwent biomechanical testing in a published study by Yildirim et al.^[2] These plates were exposed to standardized combined axial and

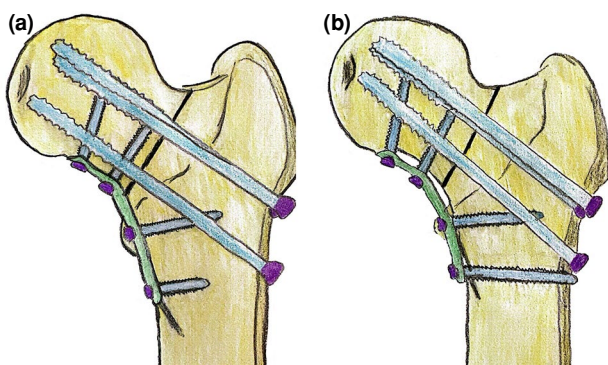


FIGURE 1. Schematic representation of medial buttress plate fixation in vertically unstable femoral neck fractures. (a) Group A construct showing a four-hole medial buttress plate positioned along the medial femoral neck, fixed with four unicortical cortical screws. (b) Group B construct in which the same plate is applied, but the most distal screw is inserted bicortically. In both configurations, three cannulated screws are placed in an inverted triangle orientation to achieve interfragmentary compression.

torsional loading protocols and were selected for microstructural evaluation based on predefined failure criteria.

All retrieved plates were analyzed using a ZEISS EVO 10 scanning electron microscope (Carl Zeiss, Wetzlar, Germany) at the Turkish Petroleum International Company Research Laboratory. Each sample was mounted on aluminum stubs using sticky carbon adhesive tapes, then transferred into the SEM vacuum chamber for imaging (Figure 2). The SEM analysis was performed using a ZEISS EVO 10 scanning electron microscope (Carl Zeiss, Wetzlar, Germany) under the following settings: an accelerated voltage of 20 kV, a beam current of 30 μ A, and a working distance ranging from 3 to 48 mm. The imaging and data acquisition were conducted using SmartSEM software (Carl Zeiss).

High-resolution micrographs were acquired from critical regions of interest, particularly the screw holes (m1 to m4) and the bent region of the plate. Structural abnormalities including plastic deformation, micro-cracks, delamination, and localized surface disruptions were documented. Comparative evaluation between the unicortical (Group A) and bicortical (Group B) fixation groups was performed to identify specific deformation patterns associated with different screw configurations.

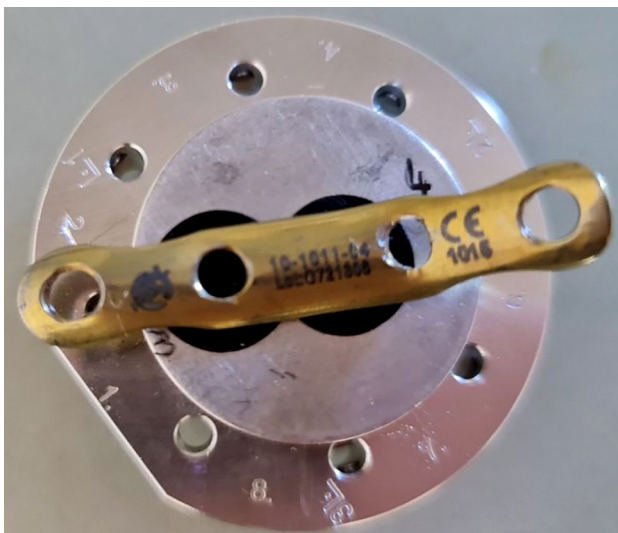


FIGURE 2. Top-down view of a medial buttress plate mounted on an aluminum SEM stub using sticky carbon adhesive tape. The plate is positioned to expose all screw holes (m1 to m4) for scanning electron microscopy.
SEM: Scanning electron microscopy.

To ensure consistency in image labeling and structural assessment, each MBP was analyzed with its screw holes sequentially labeled as m1 to m4, from proximal to distal (Figure 3). To facilitate clear identification across groups, each hole was prefixed with the group designation; e.g., A-m2 refers to the second hole of a plate from Group A, while B-m3 indicates the third hole of a Group B plate. This nomenclature was used throughout the SEM analysis to correlate specific deformation sites with experimental groups and loading configurations.

Scanning electron microscopy-Based Semi-Quantitative Scoring System

To systematically assess the deformation characteristics of MBPs following biomechanical loading, a semi-quantitative scoring system was applied based on SEM findings. Each plate was

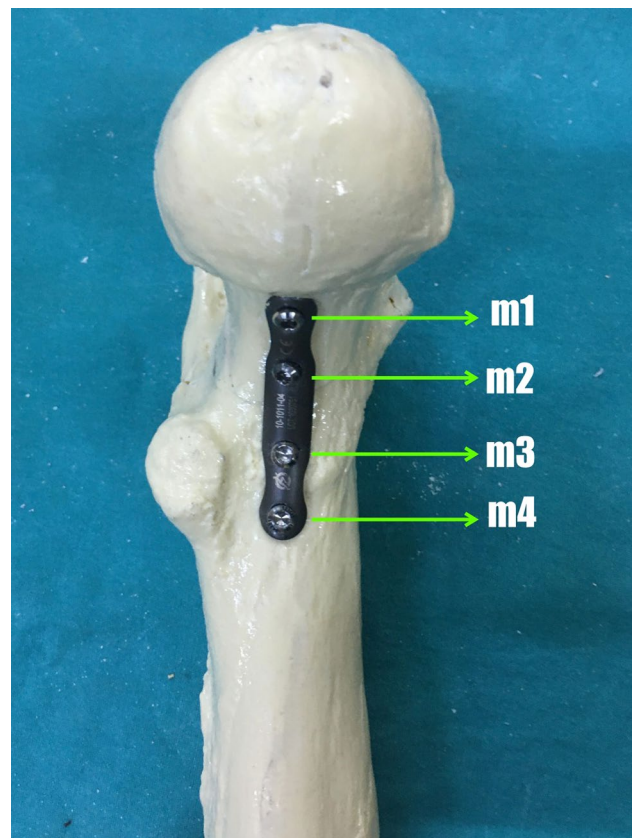


FIGURE 3. Medial view of a femoral neck model showing the screw hole labeling scheme used during SEM evaluation. The four holes on the medial buttress plate were sequentially labeled as m1 to m4 from proximal to distal, ensuring consistency in image acquisition and deformation scoring across all specimens.
SEM: Scanning electron microscopy.

Plate ID	Hole no.				Total score
	m1	m2	m3	m4	
A-1	0	1	1	0	2
A-2	0	1	1	0	2
A-3	1	1	1	0	3
A-4	0	1	1	1	3
A-5	0	1	1	0	2
B-1	0	1	1	1	3
B-2	0	2	2	0	4
B-3	0	2	2	0	4
B-4	1	2	3	1	7
B-5	0	2	1	1	4

SEM: Scanning electron microscopy.
 Scores: 0= No deformation; 1= Plastic deformation without crack; 2= Microcrack; 3= Complete fracture or structural collapse.
 Median total deformation scores were 2 in Group A and 4 in Group B; this difference was statistically significant (Mann-Whitney U=1.00, p=0.0181).

assessed at four screw hole regions (m1 to m4), and the following criteria were scored independently by a senior geological engineer with expertise in SEM-based failure analysis:

- Score 0: No deformation (smooth surface, intact margins)
- Score 1: Localized plastic deformation without evidence of cracking
- Score 2: Localized material distortion by microcracks
- Score 3: Complete fracture, plate discontinuity, or perforation with structural collapse.

The total deformation score for each plate was calculated by summing the scores of its four screw holes (maximum score per plate=12) (Table I).

Statistical analysis

Statistical analysis was performed using the IBM SPSS version 30.0 software (IBM Corp., Armonk, NY, USA). Descriptive data were expressed in median and interquartile range (IQR) or number and frequency, where applicable. Group comparisons were conducted using the Mann-Whitney U test to evaluate differences in total deformation scores between Group A and Group B plates. Intra- and inter-observer correlations were assessed using the intraclass correlation coefficients (ICCs). A *p* value of <0.05 was considered statistically significant.

RESULTS

Visual and microstructural changes observed on scanning electron microscopy

Based on SEM analysis, clear differences in microstructural deformation were observed between the two groups. Plates from Group B, in which the distal screw was placed bicortically, exhibited more severe structural changes, including localized plastic deformation, screw hole elongation, microcracks, and in some cases, complete fractures, compared to Group A, where the distal screw was unicortical.

Group A plates (A-1 to A-5) exhibited mild-to-moderate deformation, predominantly localized around the A-m2 and A-m3 screw holes. These alterations were characterized by bands of localized plastic deformation (commonly referred to as strain bands), surface irregularities, and subtle plastic flow (indicating localized permanent displacement of material under stress), without any evidence of cracks or fractures (Figure 4).

In contrast, Group B plates demonstrated more pronounced structural compromise, particularly in the midportion of the plate. Plate B-1 did not exhibit any visible fractures or cracks, but showed consistent plastic deformation across B-m2, B-m3, and B-m4 (Figure 5a). Plates B-2 and B-3 exhibited microcracks at both B-m2 and B-m3, while the

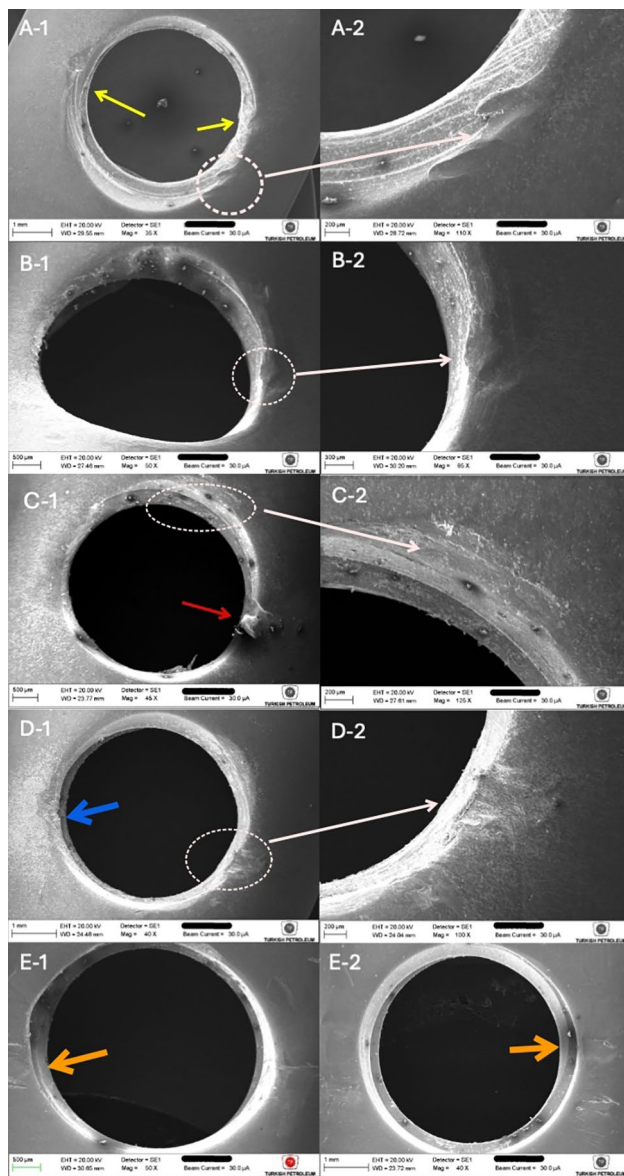


FIGURE 4. Representative SEM images showing the most deformed screw hole ("m") from each medial buttress plate in Group A (A-1 to A-5), arranged from top to bottom. Each row includes paired images of the same region at low (left) and high (right) magnification. White dotted circles and arrows indicate the specific region magnified in the corresponding right-hand image. In A-1, localized surface irregularities and strain banding are visible, as indicated by yellow arrows, without evidence of microcracks. In B-1, mild plastic deformation is noted at the screw hole edge. C-1 demonstrates prominent edge disruption with localized material loss, highlighted by the red arrow. In D-1, subtle surface abrasion and deformation are observed along the rim, as marked by the blue arrow. E-1 reveals minimal surface disruption without clear structural compromise, indicated by orange arrows. All SEM images were obtained using 20.00 kV acceleration voltage and 30.0 µA beam current. Scale bars range from 200 µm to 1 mm. SEM: Scanning electron microscopy.

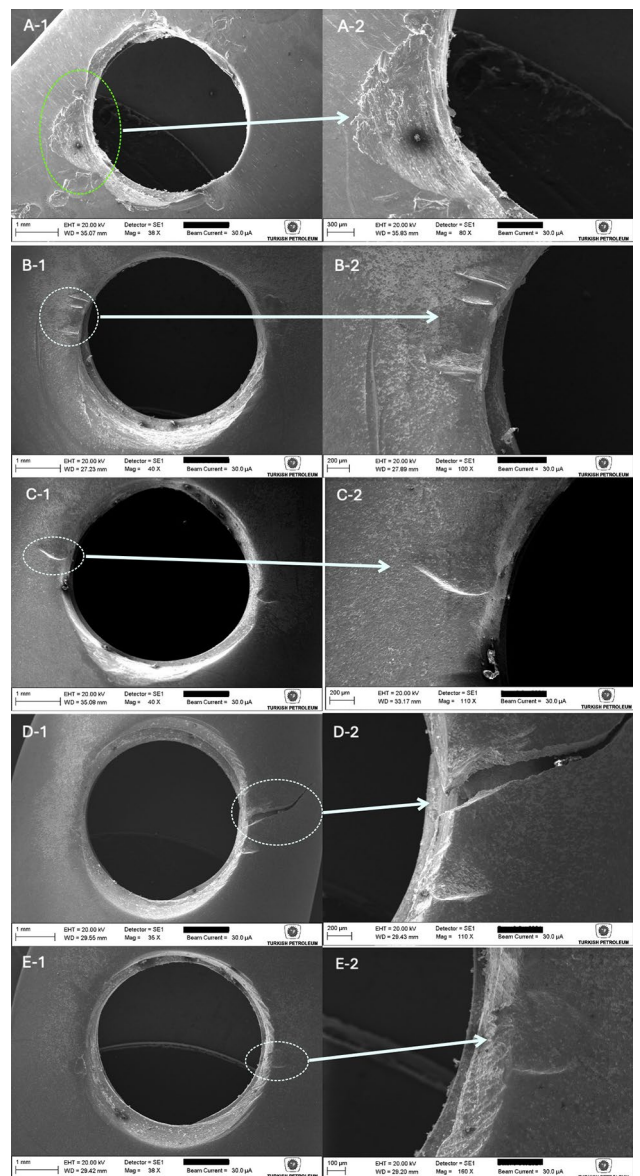


FIGURE 5. Representative SEM images showing the most deformed screw holes from each medial buttress plate in Group B (B-1 to B-5), displayed from top to bottom. Each row includes paired images from the same screw hole at low (left) and high (right) magnification. White dotted circles and arrows indicate the region of interest that has been magnified. In Plate B-1, the third hole (B-m3) demonstrates isolated plastic deformation without evidence of cracking or fracture. In Plate B-2, a distinct crack is visible at B-m3, while Plate B-3 similarly shows crack formation at the same location. Plate B-4 exhibits a complete fracture originating from B-m3, characterized by a linear cortical disruption extending radially. Finally, Plate B-5 reveals a localized crack at B-m2, without complete cortical discontinuity. All SEM images were acquired at an acceleration voltage of 20.00 kV and a beam current of 30.0 µA. Scale bars range from 200 µm to 1 mm. SEM: Scanning electron microscopy.

other screw holes showed no detectable surface damage (Figure 5b, c). Plate B-4 demonstrated the most severe findings, with a complete fracture at B-m3 (Figure 5d), a microcrack at B-m2, and plastic deformation at B-m1 and B-m4. Plate B-5 showed a deep microcrack at B-m2 and plastic deformation at B-m3 and B-m4 (Figure 5e).

Semi-quantitative analysis of SEM images revealed consistently lower deformation scores in Group A compared to Group B. The median total score was 2 (IQR: 2-3) in Group A and 4 (IQR: 4-5) in Group B. This difference was statistically significant ($p=0.0181$). The ICCs for intra- and inter-observer correlations for our SEM-Based Semi-Quantitative Scoring System were 0.89 and 0.83, respectively.

DISCUSSION

In the current study, we evaluated the deformation patterns of MBPs under combined axial and torsional loading, with a particular focus on the influence of distal bicortical screw placement. The SEM revealed significantly more microstructural damage in the bicortical fixation group, including microcracks, plastic deformation, and occasional complete fractures. These were predominantly localized in the central portion of the plate, where the implant is manually contoured to match the medial curvature of the femoral neck. This area appears to act as a mechanical weak point, vulnerable to stress concentration during physiological loading. The findings of this study may provide additional contribution to tailor implant design and guide surgical decision-making in the management of vertically unstable FNFs.

Our first hypothesis, that MBPs would maintain structural integrity while providing mechanical support, was partially supported. No complete failure was observed in the unicortical group, but structural compromise, including one complete fracture, occurred in the bicortical group. These findings suggest that, although medial plates can enhance mechanical stability, screw configuration, particularly bicortical anchorage, plays a critical role in the long-term durability of the construct. In contrast, our second hypothesis, that deformation would be concentrated around the bent region of the plate, was clearly confirmed, as damage consistently clustered in this area across both groups.

The present study builds upon our previous biomechanical analysis,^[2] showing that distal bicortical screw placement enhances axial stiffness and failure force, while inverted triangle constructs

alone provide sufficient torsional stability. By incorporating SEM, the present study reveals how screw configuration affects the material integrity of MBPs under physiological loading. To the best of our knowledge, this is the first study to directly demonstrate stress-induced microdamage associated with screw positioning. These findings complement prior mechanical data by highlighting that although bicortical fixation improves initial axial performance, it may also predispose the plate to early fatigue or failure. This concern may be especially relevant in cases of delayed union or avascular necrosis, where sustained loading persists beyond early recovery.

Previous biomechanical studies^[9,12,14] have highlighted the role of MBP in enhancing stability in vertically oriented FNFs. In a recent finite element analysis, Li et al.^[12] designed a medial anatomical buttress plate (MABP) tailored from patient-specific computed tomography (CT) scans and demonstrated superior mechanical performance compared to both cannulated screws alone and cannulated screws augmented with a one-third tubular plate. The anatomically contoured MABP distributed stress more evenly across the plate and reduced stress concentration at the screw holes. While these findings support the mechanical rationale for medial plating, the real-world applicability of such anatomical designs may be limited due to inter-individual variability in femoral neck anatomy. Our results add a critical microstructural perspective to this discourse by revealing how even standard contoured plates may accumulate stress-induced damage at the bent region, particularly when bicortical screw fixation is used.

The finding of more severe deformation and even complete fractures in the bicortical group should be regarded as a potential risk while considering this fixation strategy. From a clinical standpoint, such microdamage may predispose the construct to early plate fatigue, screw loosening, or even nonunion, particularly in cases where loading persists for prolonged periods.^[20,21] Although our findings may not directly translate into changes in clinical practice, they should highlight the need for cautious consideration when bicortical fixation is applied. These concerns may be especially relevant in scenarios such as delayed union or in young, active patients who impose higher repetitive loads on the construct. Recontouring may further compromise the structural integrity of the plate and accelerate metal degradation, thereby contributing to crack formation. In this context, the

use of anatomically contoured locking plates, tailored to the patient's specific anatomy, should be considered a more favorable fixation strategy to mitigate this risk.^[22] This consideration is particularly important in Pauwels type III FNFs, which are associated with high complication rates including nonunion, avascular necrosis of the femoral head, and overall revision rates approaching 18%.^[23]

Nevertheless, this study has several limitations. First, synthetic composite femur models were used instead of cadaveric specimens. Although these models are designed to replicate the biomechanical properties of human bone, they do not capture the microarchitectural variability of trabecular structures. However, according to a hardness test described by Rho et al.,^[18] the cancellous bone hardness ratio for the composite femur models used in this study was estimated to be 69.1%. These data demonstrate that the model used in this study is a suitable model of human bone. However, the inability to assess the clinical and toxicological effects of titanium plates remaining in the body, particularly microdamage to surrounding tissues caused by particle release at the plate-bone interface, is a major limitation of our study. Second, while the cyclic loading protocol was designed to simulate physiological conditions, it may not fully reflect the cumulative mechanical demands encountered over longer periods *in vivo*. Finally, the current analysis was limited to a single plate design; future studies incorporating various implant geometries, including anatomically contoured or locking plates, as well as long-term fatigue testing, are warranted to generalize the findings and optimize construct longevity.

In conclusion, this experimental study findings suggest that while distal bicortical screw placement can be employed to enhance initial stability in MBP in the management of Pauwels type III FNFs, it may inadvertently increase the risk of microstructural damage at the contoured central region of the plate. In our study, SEM revealed localized, stress-induced changes in this bent area, which may compromise the long-term durability of the construct, particularly under sustained mechanical loading. Based on these findings, bending the area where the screw hole is located is not recommended to preserve the mechanical strength of the plate.

Data Sharing Statement: The data that support the findings of this study are available from the corresponding author upon reasonable request.

Author Contributions: Idea/concept, references and fundings: C.Y., O.G.M.; Design, literature review: C.Y., O.G.M., Y.N.H.; Control/supervision: C.Y., O.G.M., S.E.B.; Data collection and/or processing: C.Y., O.G.M., H.C., S.E.B.; Analysis and/or interpretation: C.Y., H.C.; Writing the article: C.Y., O.G.M., H.C., M.D.; Critical review: C.Y., M.D.; Materials: C.Y., Y.N.H., H.C., S.E.B.

Conflict of Interest: The authors declared no conflicts of interest with respect to the authorship and/or publication of this article.

Funding: The authors received no financial support for the research and/or authorship of this article.

REFERENCES

1. Augat P, Bliven E, Hackl S. Biomechanics of femoral neck fractures and implications for fixation. *J Orthop Trauma* 2019;33 Suppl 1:S27-S32. doi: 10.1097/BOT.0000000000001365.
2. Yildirim C, Demirel M, Karahan G, Cetinkaya E, Misir A, Yamak F, et al. Biomechanical comparison of four different fixation methods in the management of Pauwels type III femoral neck fractures: Is there a clear winner? *Injury* 2022;53:3124-3129. doi: 10.1016/j.injury.2022.06.029.
3. Levack AE, Gausden EB, Dvorzhinskiy A, Lorich DG, Helfet DL. Novel treatment options for the surgical management of young femoral neck fractures. *J Orthop Trauma* 2019;33 Suppl 1:S33-37. doi: 10.1097/BOT.0000000000001368.
4. Slobogean GP, Sprague SA, Scott T, McKee M, Bhandari M. Management of young femoral neck fractures: Is there a consensus? *Injury* 2015;46:435-40. doi: 10.1016/j.injury.2014.11.028.
5. Tahak F, Yaka H, Kırılmaz A, Kekeç AF, Çolak TS, Özer M. Relationship between mortality and HALP score in femoral neck fractures treated with hemiarthroplasty. *Jt Dis Relat Surg* 2025;36:589-95. doi: 10.52312/jdrs.2025.2093.
6. Yang JJ, Lin LC, Chao KH, Chuang SY, Wu CC, Yeh TT, et al. Risk factors for nonunion in patients with intracapsular femoral neck fractures treated with three cannulated screws placed in either a triangle or an inverted triangle configuration. *J Bone Joint Surg Am* 2013;95:61-9. doi: 10.2106/JBJS.K.01081.
7. Bout CA, Cannegieter DM, Juttman JW. Percutaneous cannulated screw fixation of femoral neck fractures: The three point principle. *Injury* 1997;28:135-9. doi: 10.1016/s0020-1383(96)00161-1.
8. Aminian A, Gao F, Fedoriw WW, Zhang LQ, Kalainov DM, Merk BR. Vertically oriented femoral neck fractures: mechanical analysis of four fixation techniques. *J Orthop Trauma* 2007;21:544-8. doi: 10.1097/BOT.0b013e31814b822e.
9. Mir H, Collinge C. Application of a medial buttress plate may prevent many treatment failures seen after fixation of vertical femoral neck fractures in young adults. *Med Hypotheses* 2015;84:429-33. doi: 10.1016/j.mehy.2015.01.029.
10. Chan YS, Yuan LJ, Hung SS, Wang CJ, Yu SW, Chen CY, et al. Arthroscopic-assisted reduction with bilateral buttress plate fixation of complex tibial plateau fractures. *Arthroscopy* 2003;19:974-84. doi: 10.1016/j.arthro.2003.09.038.
11. Chen NC, Jupiter JB. Management of distal radial fractures. *J Bone Joint Surg Am* 2007;89:2051-62. doi: 10.2106/JBJS.G.00020.

12. Li J, Yin P, Zhang L, Chen H, Tang P. Medial anatomical buttress plate in treating displaced femoral neck fracture a finite element analysis. *Injury* 2019;50:1895-900. doi: 10.1016/j.injury.2019.08.024.
13. Liu J, Li Z, Ding J, Huang B, Piao C. Biomechanical analysis of two medial buttress plate fixation methods to treat Pauwels type III femoral neck fractures. *BMC Musculoskelet Disord* 2022;23:49. doi: 10.1186/s12891-022-05014-4.
14. Ye Y, Chen K, Tian K, Li W, Mauffrey C, Hak DJ. Medial buttress plate augmentation of cannulated screw fixation in vertically unstable femoral neck fractures: Surgical technique and preliminary results. *Injury* 2017;48:2189-93. doi: 10.1016/j.injury.2017.08.017.
15. Huang ZY, Su YH, Huang ZP, Wang YB, Du GC, Huang YP, et al. Medial buttress plate and allograft bone-assisted cannulated screw fixation for unstable femoral neck fracture with posteromedial comminution: A retrospective controlled study. *Orthop Surg* 2022;14:911-8. doi: 10.1111/os.13273.
16. Mughrabi H. Microstructural mechanisms of cyclic deformation, fatigue crack initiation and early crack growth. *Philos Trans A Math Phys Eng Sci* 2015;373:20140132. doi: 10.1098/rsta.2014.0132.
17. Giordano V, Alves DD, Paes RP, Amaral AB, Giordano M, Belangero W, et al. The role of the medial plate for Pauwels type III femoral neck fracture: A comparative mechanical study using two fixations with cannulated screws. *J Exp Orthop* 2019;6:18. doi: 10.1186/s40634-019-0187-3.
18. Rho JY, Tsui TY, Pharr GM. Elastic properties of human cortical and trabecular lamellar bone measured by nanoindentation. *Biomaterials* 1997;18:1325-30. doi: 10.1016/s0142-9612(97)00073-2.
19. Türkmen F, Kaçıra BK, Özkaya M, Erkoçak ÖF, Acar MA, Özer M, et al. Comparison of monoplanar versus biplanar medial opening-wedge high tibial osteotomy techniques for preventing lateral cortex fracture. *Knee Surg Sports Traumatol Arthrosc* 2017;25:2914-20. doi: 10.1007/s00167-016-4049-6.
20. Lee KB, Jeong SY, Kim SH, Shim DG. Complete reduction for pilon fracture can make complete failure. *J Am Podiatr Med Assoc* 2018;108:257-61. doi: 10.7547/17-001.
21. von Rüden C, Augat P. Failure of fracture fixation in osteoporotic bone. *Injury* 2016;47 Suppl 2:S3-10. doi: 10.1016/S0020-1383(16)47002-6.
22. Leuders S, Thöne M, Riemer A, Niendorf T, Tröster T, Richard HA, et al. On the mechanical behaviour of titanium alloy TiAl6V4 manufactured by selective laser melting: Fatigue re-sistance and crack growth performance. *Int J Fatigue* 2013;48:300-7.
23. Slobogean GP, Sprague SA, Scott T, Bhandari M. Complications following young femoral neck fractures. *Injury* 2015;46:484-91. doi: 10.1016/j.injury.2014.10.010.